doi:10.26443/seismica.v4i1.1430

Using citizen science Raspberry Shake seismometers to enhance earthquake location and characterisation: a case study from Wellington, New Zealand

Bethany Hughes [1], **Finnigan Illsley-Kemp** [*1], **Eleanor R. H. Mestel** [1], **John Townend** [1], **Chanthujan Chandrakumar** [2], **Raj Prasanna** [2]

[1]School of Geography, Environment and Earth Sciences, Victoria University of Wellington, Wellington, New Zealand, [2]Joint Centre for Disaster Research, Massey University, Wellington, New Zealand

Author contributions: *Conceptualization*: Finnigan Illsley-Kemp. *Methodology*: Bethany Hughes, Finnigan Illsley-Kemp, Eleanor Mestel. *Formal Analysis*: Bethany Hughes. *Resources*: Chantujan Chandrakumar, Raj Prasanna. *Writing - Original draft*: Bethany Hughes, Finnigan Illsley-Kemp. *Writing - Review & Editing*: Bethany Hughes, Finnigan Illsley-Kemp, Eleanor Mestel, John Townend, Chantujan Chandrakumar, Raj Prasanna. *Supervision*: Finnigan Illsley-Kemp, Eleanor Mestel, John Townend.

Abstract The recent development of low-cost citizen seismometers has opened new avenues for earthquake analysis. We explore the integration of Raspberry Shake citizen seismometers with the national GeoNet seismic network to improve the precision of earthquake locations in Wellington, New Zealand. We use a dataset of 19 earthquakes between magnitudes 1.1 and 3.5 and between hypocentral distances of 22 km and 102 km. Our findings demonstrate that using Raspberry Shake seismometers in conjunction with the GeoNet network is effective for both the locating and characterisation of earthquakes. Notably, we find that precise station locations are less critical for precise earthquake location, a significant factor given that the publicly available Raspberry Shake locations are obfuscated to protect user privacy. These results suggest that, dependent on network geometry, citizen seismometer data can be a valuable tool in seismic monitoring and improve earthquake location capability, whilst remaining cost-effective.

Production Editor:
Yen Joe Tan
Handling Editor:
György Hetényi
Copy & Layout Editor:
Sarah Jaye Oliva

Received:
August 19, 2024
Accepted:
December 9, 2024
Published:
February 7, 2025

1 Introduction

In recent years the advent of low-cost and low-maintenance seismic sensors has enabled citizen scientists to record seismic data at their homes. Of particular note is the "Raspberry Shake" (RS) family of seismometers, which at the time of writing has more than 2000 seismometers active around the globe. Raspberry Shake seismometers are miniature ($140 \times 135 \times 60$ mm for the RS4D) but powerful publicly available seismometers powered by Raspberry Pi hardware (Upton and Halfacree, 2016) that connect to a global seismic network (https://www.raspberryshake.org). The intention of the project is to improve global earthquake detection at a low cost ($550–$1100 USD). RS currently markets three models of seismic "shake" devices: the RS1D sensor measures the vertical component of velocity, the RS3D sensor measures all three components of velocity, and the RS4D sensor measures vertical velocity and all three components of acceleration. A fourth device, the Raspberry Boom, contains an infrasonic sensor to measure acoustic signals, and the RS&BOOM incorporates the features of both a RS1D and Raspberry Boom. The RS network has been utilised for a variety of applications, including the monitoring of rockfall, and icequakes, and identification of buildings subject to high levels of shaking (Manconi et al., 2018; Özcebe et al., 2022; Winter et al., 2021). It has also proved to be a highly effective education and outreach tool (e.g., Subedi et al., 2020)

RS seismometers pose a set of challenges for locating earthquakes. Unlike traditional seismometers that are installed in contact with the ground and in locations where there is little noise that could interfere with earthquake signals, RS installation is unregulated and chosen at the user's discretion. A RS located within a household is subjected to local signals such as washing machines which can confound recordings of earthquake signals. A RS may be installed attached to flooring or furniture, and thus not directly measure ground shaking at that location. The commonly used RS4D sensors have relatively high levels of self-noise through their internal electronics across a frequency range of 0.05–30 Hz, which can mask smaller signals and contribute to overestimation of earthquake magnitudes (Anthony et al., 2019). Another challenge with using RS data for earthquake locations is that publicly available seismometer positions are obfuscated by up to 1 km to protect user privacy. For each of the RS seismometers employed here, the precise location had been recorded during the network deployment, so we were able to locate earthquakes using the correct sensor locations. Notwithstanding these challenges, several studies have investigated the applicability of

*Corresponding author: finnigan.illsleykemp@vuw.ac.nz

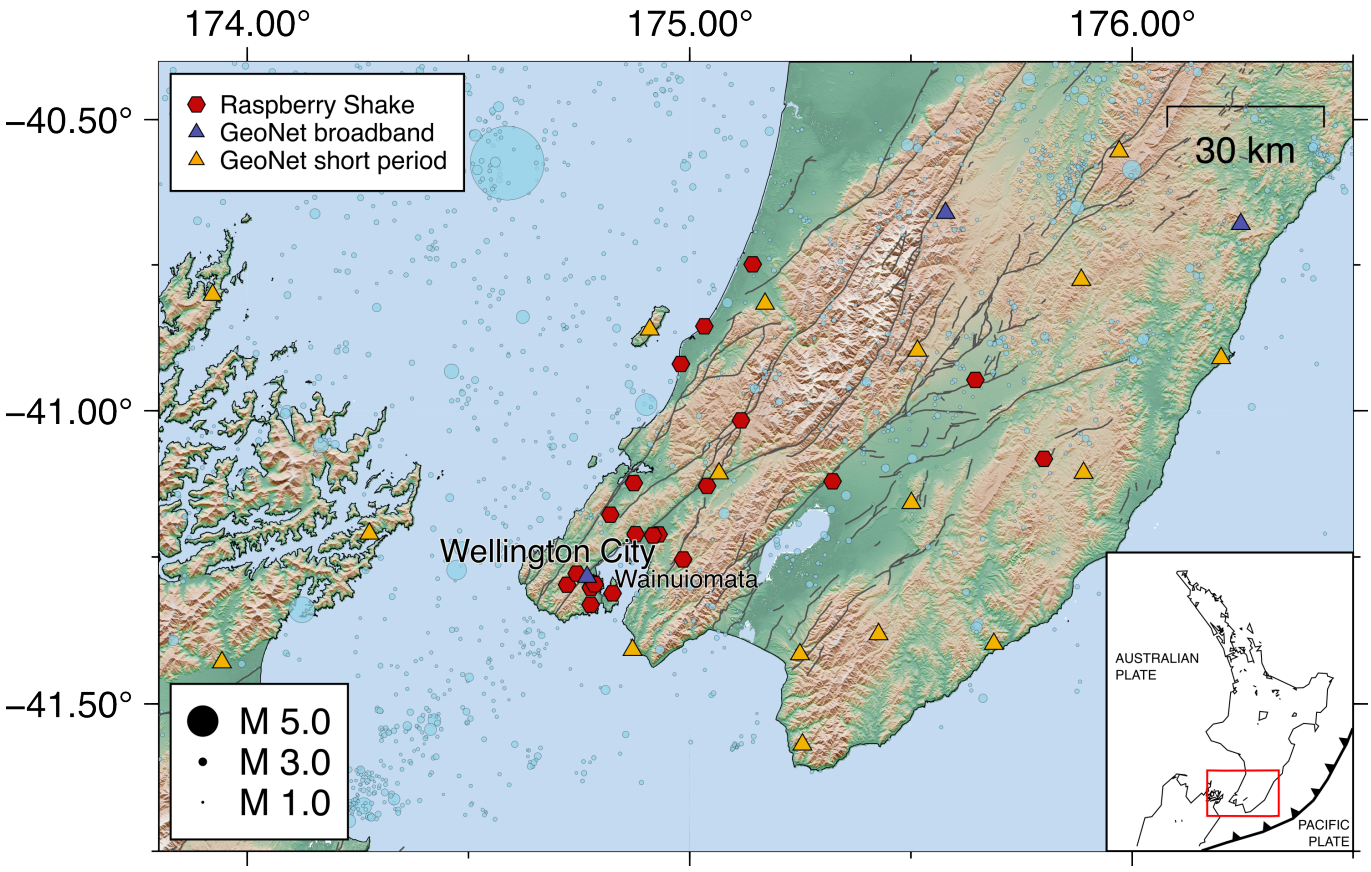

Figure 1 The seismic network in the Wellington region showing the permanent national GeoNet network (blue and orange triangles), and the citizen science Raspberry Shake network (red hexagons) used in this study. GeoNet earthquakes from 2022-12-01 and 2023-12-01 are shown in blue and sized by magnitude. Black lines denote active faults (Langridge et al., 2016) and the inset shows the study area in New Zealand.

RS seismometers to seismological research, and have concluded that they are capable of reliably estimating earthquake magnitudes (Anthony et al., 2019), detecting and locating both local earthquakes (Subedi et al., 2024) and large-magnitude mainshock-aftershock sequences (Calais et al., 2022; Paul et al., 2023), monitoring volcanic eruptions (Balangue-Tarriela et al., 2022) and induced geothermal seismicity (Holmgren and Werner, 2021). RS seismometers have also been used for less conventional seismological investigations such as monitoring African elephants (Lamb et al., 2021) and criminal forensics (Hinzen et al., 2022).

Earthquakes in New Zealand are routinely detected and located by GeoNet, using a national network of seismometers (GNS Science, 2024; Petersen et al., 2011). However, the installation and maintenance of this high-quality seismic network is expensive so the national seismic network is relatively sparse, with an average spacing of approximately 30 km in the North Island of New Zealand. In the Wellington region, there are 20 evenly distributed GeoNet seismometers (Figure 1, triangles). These GeoNet seismometers are a combination of both short period sensors (Lennartz Electronic LE-3DliteMkIII) and broadband (Streckeisen STS-6A VBB, Güralp CMG-3ESP, Nanometrics Trillium Horizon TH120-1). In this study, we used data from a high-density network of RS4D sensors in Wellington, New Zealand, to investigate whether these instruments can supplement the national seismic network in the detection, location, and characterisation of low-magnitude earthquakes. The CRISiSLab research team at Massey University, Wellington, implemented this RS seismometer network to explore the feasibility of generating Earthquake Early Warnings using low-cost MEMS-based sensors (Prasanna et al., 2022; Chandrakumar et al., 2023). This network is entirely hosted in private homes as part of a community engagement initiative. The locations of the RS seismometers are selected based on historical seismic activity recorded in and around the Wellington region over the past twenty years to generate alerts primarily for the residents of Wellington City. The deployment of this network is guided by responses from a social media campaign conducted among the Wellington community, reflecting public willingness to participate. In our study, the RS network was utilised to determine the locations of earthquakes, assessing its potential to complement the existing national seismic network. The introduction of these sensors to the pre-existing GeoNet network increases our combined network to 42 sensors. We focus here on a swarm of earthquakes detected by GeoNet beneath Wainuiomata (Figure 1). We determine earthquake locations using different configurations of the network: GeoNet stations alone, a combined network of GeoNet and RS stations, and a combined

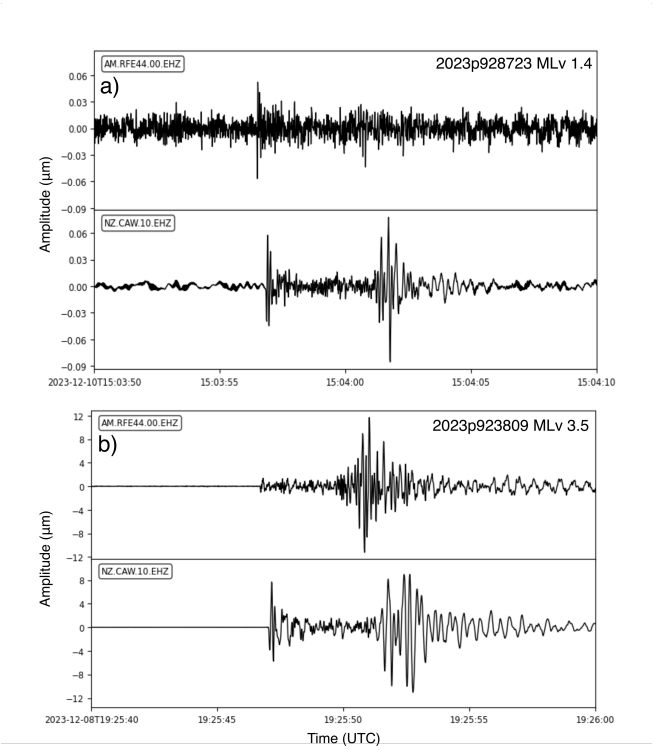

Figure 2 A waveform comparison for a) earthquake 2023p928723 (MLv 1.4) and b) earthquake 2023p923809 (MLv 3.5), both located near Wainuiomata. Both waveforms have a 1.5 Hz highpass filter applied. Top panels shows RS seismometer RFE44, 33 km away, and the bottom panels shows GeoNet seismometer CAW, 36 km away. The RS seismometer clearly shows a lower signal to noise ratio for the smaller magnitude earthquake (a), while the signal to noise ratio is high for both the RS and GeoNet seismometers in the larger magnitude earthquake (b).

network of GeoNet and obfuscated RS stations. We analyse the best-fit hypocenters and the associated probability density functions for each earthquake, as well as calculating focal mechanism solutions, with different configurations of the network to assess the performance of Raspberry Shake seismometers as a complementary network to the national network.

2 Data and methods

The network used in this study consists of the pre-existing short-period and broadband GeoNet network (Petersen et al., 2011) over the greater Wellington region and northern South Island. The study area is between the latitudes of −40.5° and −41.6°, and between the longitudes of 173.5° and 176.5°, and between depths of 0 km and 40 km. Raspberry Shake seismometers within the study area were used to augment the permanent GeoNet network, expanding the network from 20 stations to 42 stations (Figure 1). These RS seismometers used the Network Time Protocol (NTP) and were predominantly installed on the floors of single-level homes. The 20 GeoNet stations in the network are distributed with spacings of 15–50 km, and all stations are on land. The nature of the RS network comprising citizen seismometers renders the spacing of stations irregular and concentrated in the more populated urban areas. 36% of the RS seismometers within our network lie within the bounds of Wellington City, where only one GeoNet station (WEL) is located (Figure 1).

We used waveform data from each station from 2023-12-07 00:00:00 UTC and 2023-12-13 00:00:00 UTC. With all available RS seismometers being equipped with a vertical velocity sensor, all picks on both RS and GeoNet waveforms were made on the vertical component. We used the *Snuffler* toolbox from *Pyrocko* (Heimann et al., 2019) to manually pick *P*- and *S*-wave arrival-times and first-motion polarities across the network. Picks were only made on stations where the arrival-time could be identified with confidence, based on analyst experience. Poor signal-to-noise ratios made picking on RS waveforms more challenging than on GeoNet stations, particularly for small (M<2) magnitude earthquakes (Figure 2a). However for larger earthquakes the signal on RS seismometers is clear (Figure 2b). All picks were made without filtering, then stations with no picks were reviewed with variable bandpass filtering. Picks were then manually associated with each unique earthquake.

To examine the effect of using obfuscated sensor locations on earthquake locations, we located the same catalogue of earthquakes with the publicly available RS station locations. Through checking residuals, we were able to identify anomalous picks and either remove or reassess the pick, and were able to verify that picks made on obfuscated RS stations were usable for locations (Figure 3). Hypocenters were computed using *NonLinLoc*, a non-linear earthquake location programme (Lomax et al., 2000), with the IASP91 velocity model (Kennett and Engdahl, 1991) used by GeoNet for routine earthquake locations nationwide. We use a pick uncertainty of 0.5 s for both P- and S-wave picks on both sensor types. Once hypocenters had been computed, focal mechanism solutions were calculated using *MTFit* (Pugh and White, 2018) and first-motion polarities, with the azimuths and take-off angles obtained with *NonLinLoc*.

3 Results

The final catalogue consists of the 19 earthquakes detected by GeoNet in the Wellington region between 2023-12-07 00:00:00 UTC and 2023-12-13 00:00:00 UTC, located with both RS and GeoNet stations (Figure 4). Hypocentral probability density functions (PDFs) were calculated for each earthquake using: 1) GeoNet stations alone, 2) the combined network of GeoNet stations and precise RS station locations, and 3) the combined network of GeoNet stations and publicly available obfuscated RS station locations. A total of 651 arrivals (388 *P*-picks, 262 *S*-picks) were used to create the catalogue. 235 of the total picks (146 *P*-picks, 89 *S*-picks) were made on RS stations, and 416 picks (242 *P*-picks, 174 *S*-picks) were made on

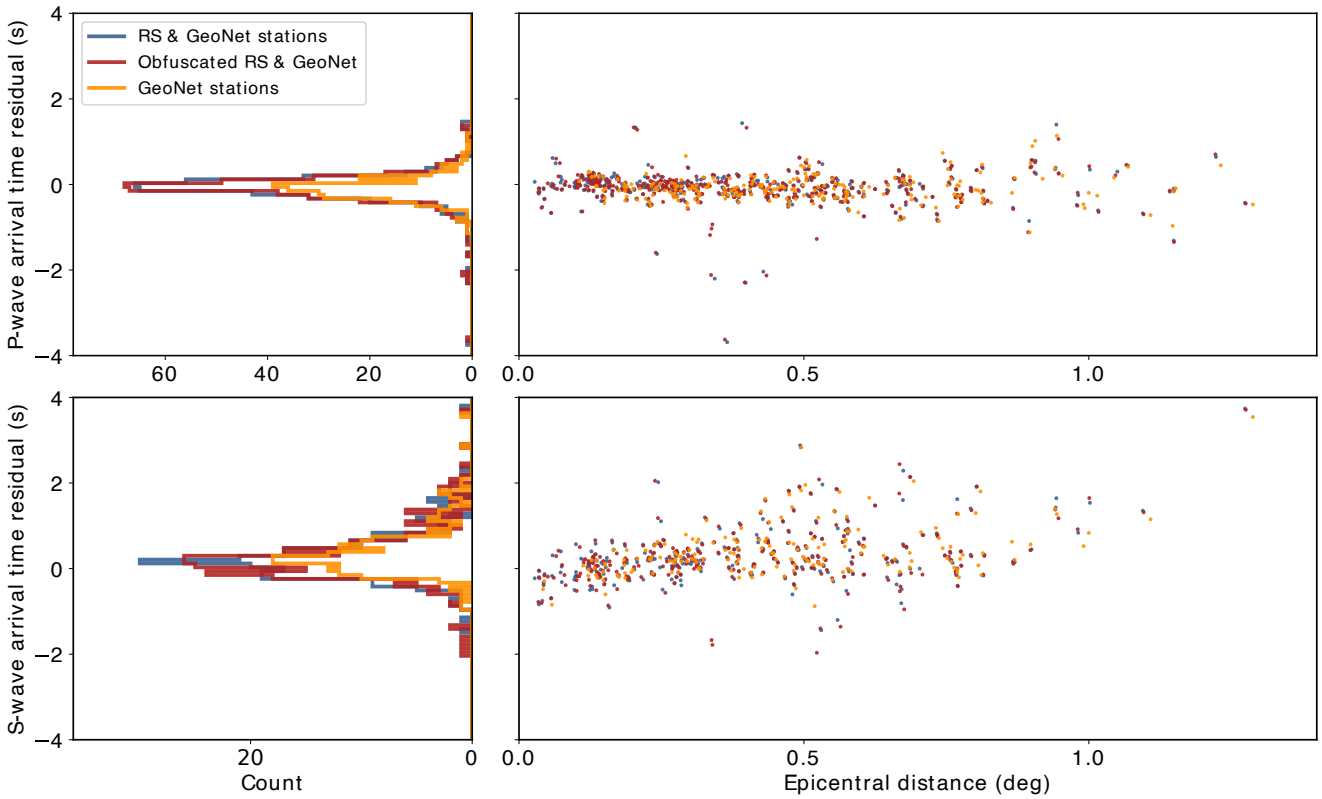

Figure 3 A comparison of travel-time residuals for earthquakes when using GeoNet stations alone (gold), the combined network of GeoNet stations and RS stations with precise locations (blue), and the combined network of GeoNet stations and obfuscated RS stations (red).

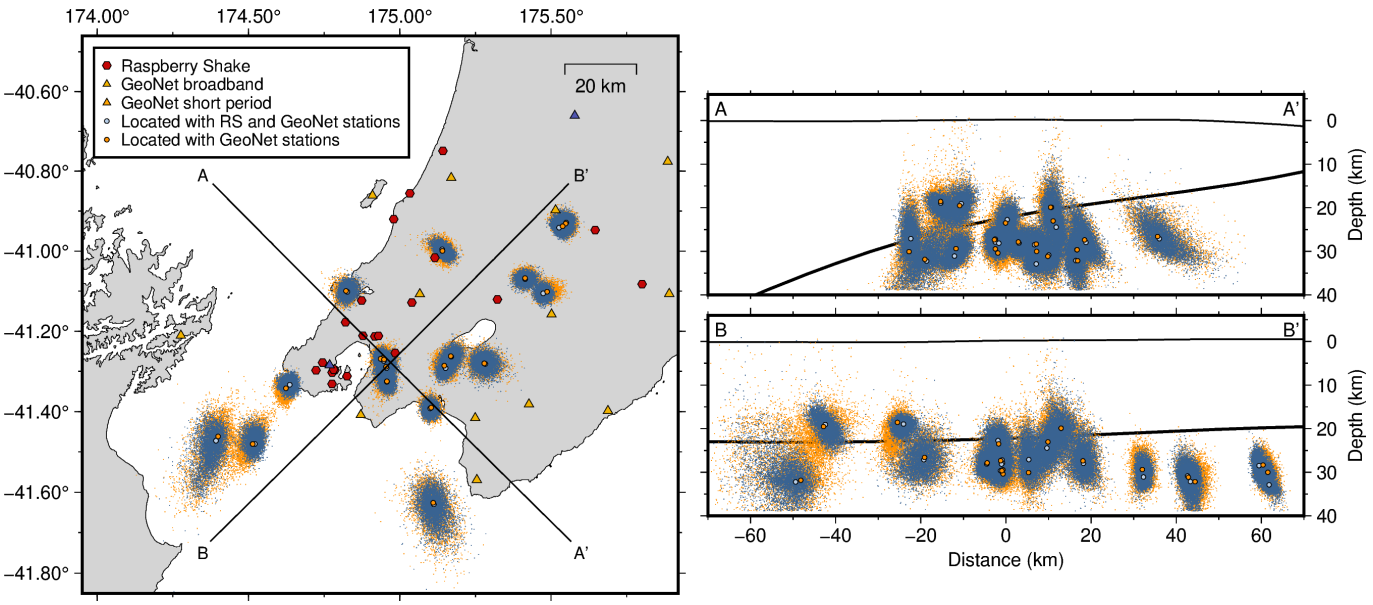

Figure 4 Hypocentral PDFs of earthquakes in the catalogues located using GeoNet stations (gold) and the combined network of GeoNet stations and RS stations with precise locations (blue). The black line illustrated in the A–A' and B–B' vertical cross-sections represents the interface between the subducting Pacific plate and Australian plate (Williams et al., 2013).

GeoNet stations. The earthquake with the largest number of picks was GeoNet earthquake 2023p923809 (https://www.geonet.org.nz/earthquake/2023p923809) with 37 *P*-picks (18 RS, 19 GeoNet) and 35 *S*-picks (19 RS, 16 GeoNet). The mean number of RS stations used per earthquake was 7, and for GeoNet stations it was 12.

We explored the quality of the *NonLinLoc* earthquake locations using the distribution of the PDFs, 1σ depth uncertainty, and the dimensions of the 1σ horizontal uncertainty ellipse for each earthquake. The lengths of the long and short axes were used to describe the uncertainty ellipse and indicate the non-spherical nature of the location uncertainties. We sampled 10000 scatter

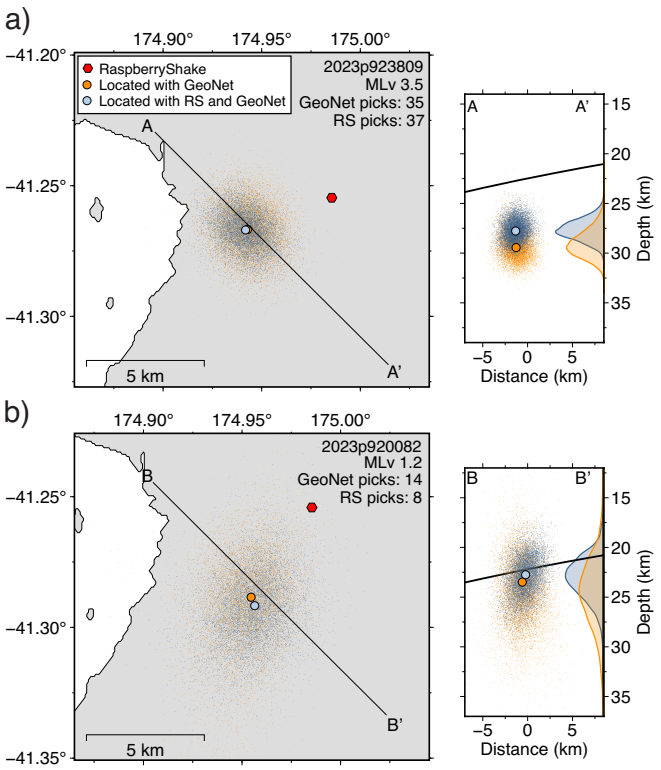

Figure 5 A comparison between earthquake location uncertainties for earthquakes 2023p923809 (top) and 2023p920082 (bottom), both beneath Wainuiomata, when using the GeoNet network (orange) and the combined network of GeoNet station and RS stations with precise locations (blue). Scatter points denote probability distribution. Cross sections show the modelled surface of the subducting Hikurangi slab (Williams et al., 2013).

points from the PDF to visualise the uncertainty cloud (Figure 4). A widespread scatter represents a poorly constrained earthquake, while tight scatter represents a well-constrained earthquake (Lomax et al., 2009).

We located the five GeoNet archived earthquakes in the Wainuiomata cluster with a range of GeoNet local magnitudes measured on the vertical component (MLv) of 1.2–3.5. The earthquakes were located using GeoNet stations alone, and with the combined network of GeoNet stations and RS stations with precise locations. When located with the combined network, the uncertainty ellipse associated with the MLv 3.5 earthquake (www.geonet.org.nz/earthquake/2023p923809) is ±1.4 km in the long axis and ±1.1 km in the short axis, with a depth uncertainty of ±1.1 km (Figure 5a). This earthquake was located with 37 *P*-picks and 35 *S*-picks. When located with GeoNet stations alone (19 *P*-picks and 16 *S*-picks), the uncertainty ellipse is ±1.6 km in the long axis and ±1.4 km in the short axis, with a depth uncertainty of ±1.4 km. In comparison, the uncertainty ellipse of a nearby (3 km away) MLv 1.2 earthquake (www.geonet.org.nz/earthquake/2023p920082) is ±2.4 km in the long axis and ±1.6 km in the short axis, with a depth uncertainty of ±2.0 km when located with the combined network (Figure 5b). This earthquake was located with 12 *P*-picks and 10 *S*-picks. When

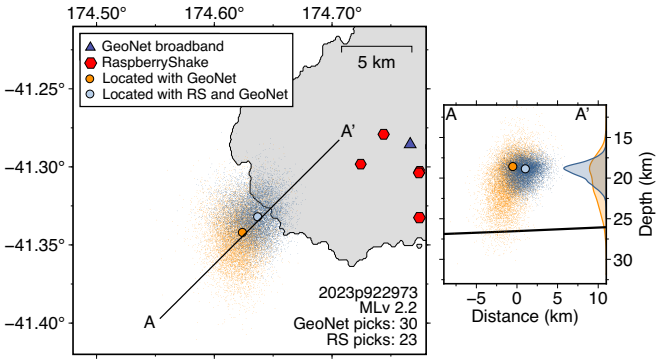

Figure 6 A comparison between earthquake location uncertainty for earthquake 2023p922973 when using the GeoNet network (orange) and the GeoNet and RS combined network (blue). Scatter points denote probability distribution. Cross sections show the modelled surface of the subducting Hikurangi slab (Williams et al., 2013).

located with GeoNet stations alone, with 8 *P*-picks and 6 *S*-picks, the uncertainty ellipse is ±3.7 km in the long axis and ±1.9 km in the short axis, with a depth uncertainty of ±3.5 km. Both earthquakes see an improvement in location confidence with the addition of RS stations, regardless of the magnitude of the earthquake. The mean reduction of uncertainty over all five earthquakes in the cluster is 12% in the short axis, 16% in the long axis, and 26% in depth uncertainty.

We explored the variation in hypocentral location and PDF distribution of an earthquake located beneath the south coast of Wellington (Figure 6). This MLv 2.2 earthquake (www.geonet.org.nz/earthquake/2023p922973) was located with 17 GeoNet *P*-picks, 13 GeoNet *S*-picks, 15 RS *P*-picks, and 8 RS *S*-picks. The uncertainty ellipse when located with the combined network is ±2.0 km in the long axis, ±1.8 km in the short axis, with a depth uncertainty of ±1.2 km. When located with GeoNet stations alone, the maximum uncertainty is ±2.7 km, minimum uncertainty is ±1.8 km, and depth uncertainty is ±2.8 km. This shows that the inclusion of RS data significantly improves the location accuracy for this earthquake.

The hypocenter location and uncertainty of the same earthquake is only slightly altered by the use of the GeoNet network in conjuction with the RS network with obfuscated locations, as opposed to true locations (Figure 7). With the combined network of GeoNet stations and obfuscated RS stations, the uncertainty ellipse of the earthquake is ±2.1 km in the long axis, ±1.8 km in the short axis, with a depth uncertainty of ±1.2 km.

Focal mechanism solutions could be computed for seven of the 19 earthquakes located. Two of these earthquakes yielded a focal mechanism solution with data from both the combined network and the GeoNet network alone. Five earthquakes yielded focal mechanism solutions only when using the combined network. A total of 98 polarity picks were used to create focal

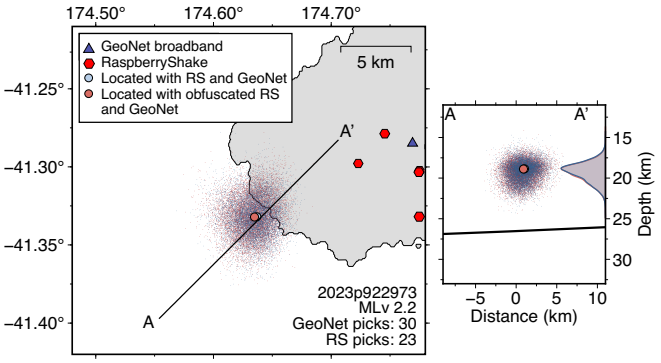

Figure 7 A comparison between earthquake location uncertainty for earthquake 2023p922973 when using the GeoNet and RS combined network with precise RS station locations (blue) and obfuscated RS station locations (red). Cross sections show the modelled surface of the subducting Hikurangi slab (Williams et al., 2013).

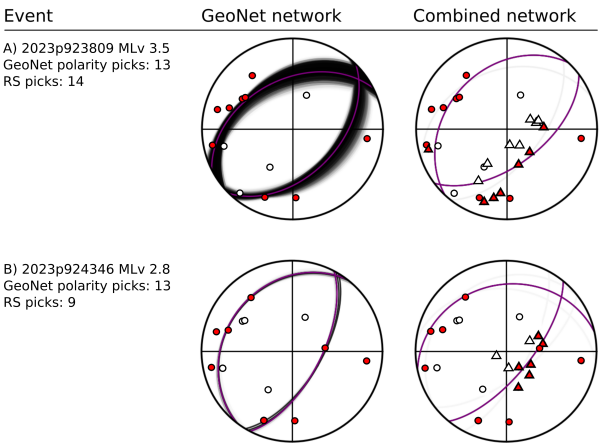

Figure 8 Focal mechanism solutions for earthquakes in the Wainuiomata cluster produced using first-motion polarities from the Raspberry Shake stations (triangles) and GeoNet network (circles). Dilitational picks are in white, and compressional picks are in red. Possible nodal planes are shown in gray, the highest probability nodal plane is shown in purple.

mechanisms, 64 of these determined from GeoNet waveforms and 34 from RS waveforms. The earthquake with the most polarity picks was GeoNet earthquake 2023p923809 (MLv 3.5) with 14 GeoNet picks and 16 RS polarity picks. Focal mechanism solutions using GeoNet stations alone and the combined network were obtained for two earthquakes in the Wainuiomata cluster (Figure 8). These focal mechanisms revealed predominantly NE–SW-orientated normal faulting. The RS polarity picks are consistent with those from GeoNet stations and maintain the general geometry of the focal mechanism, however the increased density of data points better constrains the nodal planes.

4 Discussion

In this study, we aimed to evaluate whether Raspberry Shake seismometers can complement the national seismic network for earthquake location and characterisation. We used one week of seismic data from a network of 20 GeoNet stations and 22 RS stations in the Wellington region to locate 19 earthquakes of magnitudes up to 3.5. We compared the location uncertainties when located with the combined network to those located with GeoNet stations alone. Additionally, we compared hypocentral uncertainties when located with precise RS station locations to those with publicly available, obfuscated RS station locations.

By comparing the distribution of PDFs, 1σ horizontal confidence ellipses, and depth errors associated with earthquake locations, our testing finds the addition of RS to the GeoNet network improves the accuracy of earthquake locations. For each earthquake, the PDF scatter clouds are more tightly clustered when located with the combined network. Over our entire catalogue, the mean reduction of uncertainty is 14% on the long axes and 19% on the short axes of the confidence ellipse with the addition of RS stations, and the mean reduction in depth error is 20%. This is attributed to the improved spatial coverage provided by the addition of RS to the network, and can significantly improve our understanding of these earthquakes. For an earthquake located at 20 km depth beneath the south coast of Wellington, we find a 56% reduction in the 1σ depth uncertainty, likely attributed to the high density of RS stations located nearby in Wellington City. The PDF of the earthquake when located by GeoNet stations alone intersects with the subsection interface, so there is little certainty of the earthquake source mechanism. The PDF cloud of the combined network location is entirely above the subduction interface, constraining the earthquake to the upper plate (Figure 6).

We also compared the amplitude of earthquake arrivals at both the Raspberry Shake and GeoNet sensors after removing individual instrument responses. This showed that for comparable hypocentral distances, the amplitudes measured at Raspberry Shake sensors were comparable to those at GeoNet sensors (Figure 9). This suggests that Raspberry Shake sensors can also be used to support the estimation of earthquake magnitudes for local seismicity such as that shown in this study. Finally, we investigated the viability of using RS stations to constrain focal mechanisms. The comparatively low signal-to-noise ratio in RS waveforms often makes it difficult to obtain polarity picks, especially for low-magnitude and distant earthquakes. Nevertheless, when polarity picks can be successfully obtained, we find the picks are consistent in polarity with those of GeoNet stations, and that the addition of RS stations refines the focal mechanism solutions (Figure 8). The quality of a focal mechanism is influenced by both the density and distribution of stations around the hypocenter, where a variety of take-off angles and azimuths can be obtained. Because the locations of RS stations in the Wellington region are concentrated in urban areas, the range of azimuths and take-off angles is limited when an earthquake is located outside of the

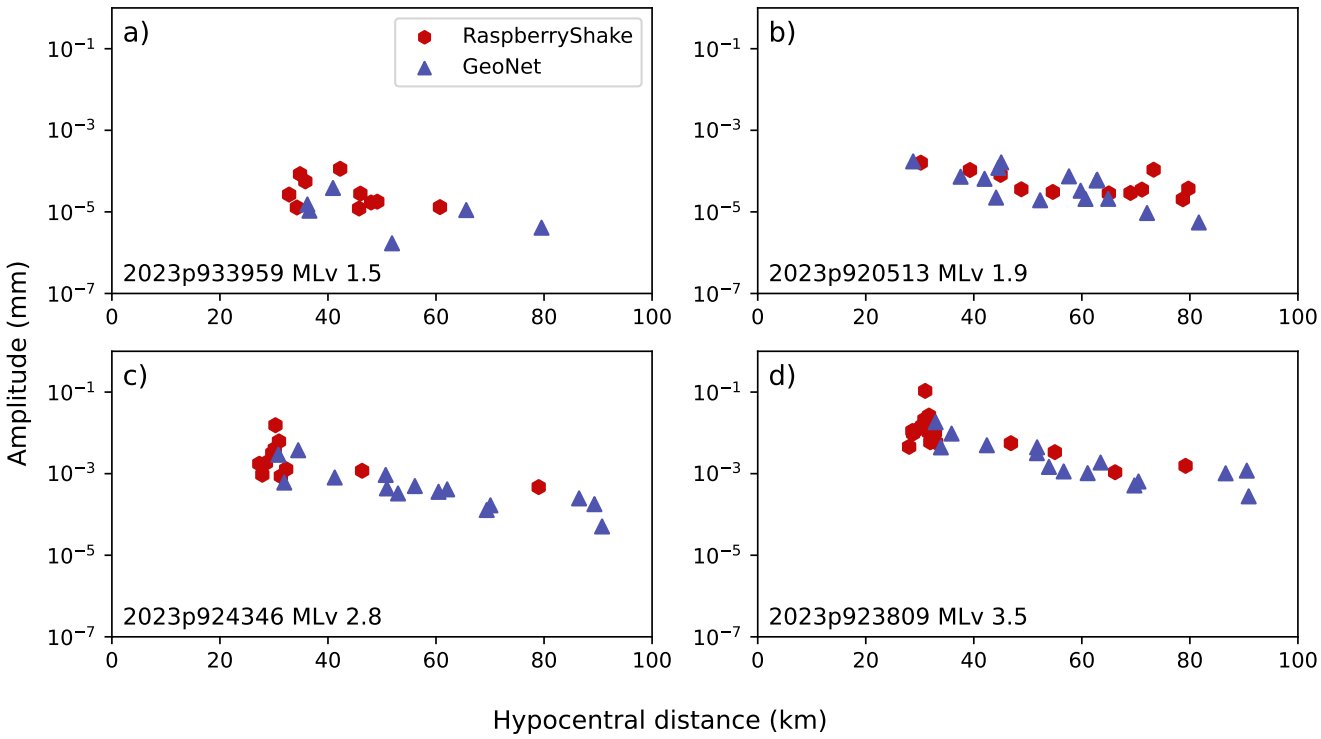

Figure 9 A comparison between amplitudes measured for four earthquakes on the vertical component of both Raspberry Shake and GeoNet seismometers. This shows there is good agreement between different sensor types and that Raspberry Shake can be used to estimate earthquake magnitudes.

RS network. However, the RS network complements the GeoNet network, which offers a broader range of azimuths and take-off angles, and provides dense coverage in its respective area of the focal sphere. In the instance of the Wainuiomata cluster, the SE-dipping nodal plane of the obtained focal mechanism solution coincides with the cluster of stations in Wellington City, allowing for the plane to be better constrained with the combined network (Figure 8).

GeoNet reported a moment tensor solution for earthquake 2023p923809 (Ristau, 2013). This solution was obtained using seven GeoNet stations, and suggests the earthquake occurred at a depth of 4 km based on variance reduction (Figure 10b). The moment tensor solution at this depth is a NE-SW-oriented reverse mechanism. Our combined network locates the same earthquake at a depth of 28 km with a NE-SW-oriented normal mechanism (Figure 10a). Our assigned depth approximately corresponds to a second peak in the variance reduction curve reported by GeoNet and the focal mechanism we obtain is similar to the GeoNet moment tensor solution for the earthquake if it were to have occurred at this depth (Figure 10b). This suggests that the combined network has better constrained the depth of the earthquake, changing the ray take-off angles and improving the focal mechanism solution for the earthquake. Disparities in velocity models and methodology may further explain variations between the routine GeoNet moment tensor solution and our own.

4.1 Limitations

A limitation of using RS seismometers for earthquake locating and characterisation is the unavailability of precise station locations from the Raspberry Shake FDSN. The distance that each station location is altered is not publicly available, though understood to be around 1 km. With our network, the median distance that station locations are altered by is 0.9 km, with a maximum of 6.8 km and a minimum of 0.2 km. However, through comparing best-fit hypocenters and PDFs of all earthquakes located by our combined network with precise station locations and the same earthquakes located with the obfuscated station locations available through the Raspberry Shake FDSN, we find that the precision of the station location does not significantly impact the best-fit location nor its uncertainty. We illustrate this with an earthquake on the south coast of Wellington (Figure 7), the hypocenter location is only shifted by 0.03 km, and uncertainty reduced by only 2%. This means that it may be possible for other researchers to integrate RS data into their analysis without knowing precise station locations, though this will be dependent on network geometry and earthquake location errors will be underestimated.

Despite the capability of improving earthquake locations and characterisation with a combined network, it is important to consider the limitations of RS seismometers. RS are not as robust as conventional seismometers; the comparatively higher self-noise levels and limited instalment regulation impact the overall quality of the RS network. Obscured station locations further compli-

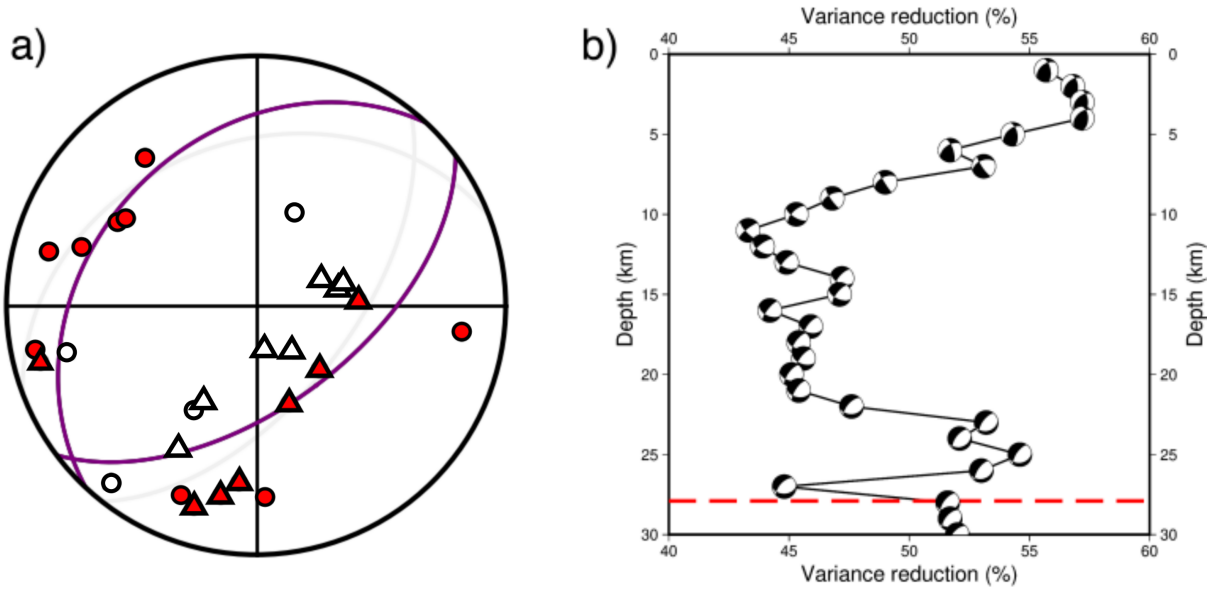

Figure 10 a) Shows the focal mechanism solutions produced using first-motion polarities from the Raspberry Shake stations (triangles) and GeoNet network (circles) for earthquake 2023p923809. Dilitational picks are in white, and compressional picks are in red. Possible nodal planes are shown in gray, the highest probability nodal plane is shown in purple. b) Shows the variance reduction with depth for moment tensor solutions calculated by GeoNet (Ristau, 2013). This shows that at depths which match the maximum likelihood hypocentre we calculate (dashed red line, 27.9 km), the moment tensor solutions are in agreement with that shown in panel a.

cate their use for earthquake location if the uncertainty in station locations exceeds the uncertainty in earthquake location. The devices are easily removed and deployed elsewhere under the same serial number, so it is important to check metadata for changes in site locations before using in analyses. Finally, when using RS for earthquake analyses, proper practice should include using vertical component data to remove any errors associated with possible horizontal component misorientation, checking arrival-time residuals for anomalous residuals that might suggest the true station location is far away, and requesting site information.

5 Conclusions

Raspberry Shake seismometers are miniature but powerful citizen seismometers powered by Raspberry Pi, with the potential to improve seismic studies. We investigated the performance of the RS network in Wellington, New Zealand at improving earthquake locations and characterisation when integrated with the national permanent GeoNet network. Our findings indicate that, despite the lower sensitivity of the RS sensors, the combined network improves both location certainty and focal mechanism solutions. Furthermore, while the precise locations of RS stations are obfuscated to protect user privacy, this does not significantly compromise the accuracy of earthquake locations. Ultimately we find that with careful checking of metadata and data quality, researchers can effectively integrate RS data into their seismic studies. Furthermore, incorporating citizen seismic networks like RS to national seismic networks can improve our understanding of earthquake dynamics.

Acknowledgements

BH, FIK, ERHM, and JT are funded by the Toka Tū Ake Natural Hazards Commission (NHC) Programme in Earthquake Seismology and Tectonic Geodesy at Victoria University of Wellington. BH is also supported by the New Zealand Ministry of Business, Innovation and Employment (Grant C05X1904 'Geothermal: the Next Generation'), and the Rachael Westegaard Memorial Masters Scholarship in Geophysics at VUW. FIK is also supported by the Marsden Fund of the Royal Society of New Zealand (Grant MFP-VUW2109 and MFP-UOA2220). CC and RP are supported by the Resilience to Nature's Challenges-Urban Theme 2020 and QuakeCoRE - IP4: Harnessing Disruptive Technologies for Seismic Resilience. GeoNet and its sponsors Toka Tū Ake NHC, GNS Science, LINZ, NEMA and MBIE are thanked for providing data used in this study. We also thank two anonymous reviewers and the editor, György Hetényi, for their constructive comments.

Data and code availability

The earthquake catalogues produced in this study are available at https://doi.org/10.5281/zenodo.13345950. All waveform data from GeoNet stations are available from GeoNet (GNS Science, 2021). All waveform data from the Raspberry Shake sensors are available from the EarthScope Data Centre (Raspberry Shake, 2016). For privacy reasons the true locations of the RS sensors are not made available. Figures were made with GMT6 (Wessel et al., 2019) and PyGMT (Tian et al., 2023). Seismic data was analysed with Pyrocko (Heimann et al., 2019) and Obspy (Beyreuther et al., 2010).

Competing interests

The authors have no competing interests.

References

Anthony, R. E., Ringler, A. T., Wilson, D. C., and Wolin, E. Do low-cost seismographs perform well enough for your network? An overview of laboratory tests and field observations of the OSOP Raspberry Shake 4D. *Seismological Research Letters*, 90 (1):219–228, 2019. doi: https://doi.org/10.1785/0220180251.

Balangue-Tarriela, M., Lagmay, A., Sarmiento, D., Vasquez, J., Baldago, M., Ybañez, R., Ybañez, A., Trinidad, J., Thivet, S., Gurioli, L., et al. Analysis of the 2020 Taal Volcano tephra fall deposits from crowdsourced information and field data. *Bulletin of Volcanology*, 84(3):35, 2022. doi: https://doi.org/10.1007/s00445-022-01534-y.

Beyreuther, M., Barsch, R., Krischer, L., Megies, T., Behr, Y., and Wassermann, J. ObsPy: a Python toolbox for seismology. *Seismological Research Letters*, 81:530–533, 2010. doi: https://doi.org/10.1785/gssrl.81.3.530.

Calais, E., Symithe, S., Monfret, T., Delouis, B., Lomax, A., Courboulex, F., Ampuero, J. P., Lara, P. E., Bletery, Q., Chèze, J., et al. Citizen seismology helps decipher the 2021 Haiti earthquake. *Science*, 376(6590):283–287, 2022. doi: https://doi.org/10.1126/science.abn1045.

Chandrakumar, C., Tan, M. L., Holden, C., Stephens, M. T., and Prasanna, R. Performance analysis of P-wave detection algorithms for a community-engaged earthquake early warning system–a case study of the 2022 M5. 8 Cook Strait earthquake. *New Zealand Journal of Geology and Geophysics*, pages 1–16, 2023. doi: https://doi.org/10.1080/00288306.2023.2284276.

GNS Science. GeoNet Aotearoa New Zealand Seismic Digital Waveform Dataset [Dataset], 2021. doi: https://doi.org/10.21420/G19Y-9D40.

GNS Science. GeoNet Aotearoa New Zealand Earthquake Catalogue, 2024. doi: 10.21420/0S8P-TZ38.

Heimann, S., Kriegerowski, M., Isken, M., Nooshiri, N., Steinberg, A., Sudhaus, H., Vasyura-Bathke, H., and Dahm, T. Pyrocko-A versatile software framework for seismology. In *Geophysical Research Abstracts*, volume 21, 2019.

Hinzen, K.-G., Krummel, H., Weber, B., and Fleischer, C. Forensic view on two Raspberry Shake burglargrams. *Journal of Seismology*, 26(5):863–873, 2022. doi: https://doi.org/10.1007/s10950-022-10098-5.

Holmgren, J. M. and Werner, M. J. Raspberry shake instruments provide initial ground-motion assessment of the induced seismicity at the united downs deep geothermal power project in Cornwall, United Kingdom. *The Seismic Record*, 1(1):27–34, 2021. doi: https://doi.org/10.1785/0320210010.

Kennett, B. L. N. and Engdahl, E. R. Traveltimes for global earthquake location and phase identification. *Geophysical Journal International*, 105:429–465, 1991. doi: https://doi.org/10.1111/j.1365-246X.1991.tb06724.x.

Lamb, O. D., Shore, M. J., Lees, J. M., Lee, S. J., and Hensman, S. M. Assessing raspberry shake and boom sensors for recording African elephant acoustic vocalizations. *Frontiers in Conservation Science*, 1:630967, 2021. doi: https://doi.org/10.3389/fcosc.2020.630967.

Langridge, R. M., Ries, W. F., Litchfield, N. J., Villamor, P., Van Dissen, R. J., Barrell, D. J. A., Rattenbury, M., Heron, D. W., Haubrock, S., Townsend, D. B., et al. The New Zealand active faults database. *New Zealand Journal of Geology and Geophysics*, 59(1):86–96, 2016. doi: https://doi.org/10.1080/00288306.2015.1112818.

Lomax, A., Virieux, J., Volant, P., and Berge-Thierry, C. *Probabilistic earthquake location in 3D and layered models: introduction of a Metropolis-Gibbs method and comparison with linear locations*, pages 101–134. Springer, Dordrecht, Netherlands, 2000. doi: https://doi.org/10.1007/978-94-015-9536-0_5.

Lomax, A., Michelini, A., and Curtis, A. *Earthquake location, direct, global-search methods*, pages 2449–2473. Springer, New York, New York, USA, 2009. doi: http://dx.doi.org/10.1007/978-0-387-30440-3.

Manconi, A., Coviello, V., Galletti, M., and Seifert, R. Monitoring rockfalls with the Raspberry Shake. *Earth Surface Dynamics*, 6 (4):1219–1227, 2018. doi: https://doi.org/10.5194/esurf-6-1219-2018.

Özcebe, A. G., Tiganescu, A., Ozer, E., Negulescu, C., Galiana-Merino, J. J., Tubaldi, E., Toma-Danila, D., Molina, S., Kharazian, A., Bozzoni, F., et al. Raspberry shake-based rapid structural identification of existing buildings subject to earthquake ground motion: The case study of Bucharest. *Sensors*, 22(13): 4787, 2022. doi: https://doi.org/10.3390/s22134787.

Paul, S., Monfret, T., Courboulex, F., Chèze, J., Calais, E., Julien Symithe, S., Deschamps, A., Peix, F., Ambrois, D., Martin, X., et al. Monitoring of local earthquakes in Haiti using low-cost, citizen-hosted seismometers and regional broadband stations. *Seismological Research Letters*, 94(6):2725–2739, 2023. doi: https://doi.org/10.1785/0220230059.

Petersen, T., Gledhill, K., Chadwick, M., Gale, N. H., and Ristau, J. The New Zealand national seismograph network. *Seismological Research Letters*, 82:9–20, 2011. doi: https://doi.org/10.1785/gssrl.82.1.9.

Prasanna, R., Chandrakumar, C., Nandana, R., Holden, C., Punchihewa, A., Becker, J. S., Jeong, S., Liyanage, N., Ravishan, D., Sampath, R., et al. "Saving Precious Seconds"—A novel approach to implementing a low-cost earthquake early warning system with node-level detection and alert generation. In *Informatics*, volume 9, page 25. MDPI, 2022. doi: https://doi.org/10.3390/informatics9010025.

Pugh, D. and White, R. MTfit: A Bayesian approach to seismic moment tensor inversion. *Seismological Research Letters*, 89(4): 1507–1513, 2018. doi: https://doi.org/10.1785/0220170273.

Raspberry Shake. Raspberry Shake [Dataset], 2016. doi: https://doi.org/10.7914/SN/AM.

Ristau, J. Update of regional moment tensor analysis for earthquakes in New Zealand and adjacent offshore regions. *Bulletin of the Seismological Society of America*, 103(4):2520–2533, 2013. doi: https://doi.org/10.1785/0120120339.

Subedi, S., Hetényi, G., Denton, P., and Sauron, A. Seismology at school in Nepal: A program for educational and citizen seismology through a low-cost seismic network. *Frontiers in Earth Science*, 8:73, 2020. doi: https://doi.org/10.3389/feart.2020.00073.

Subedi, S., Hetényi, G., Frédérick, M., Adhikari, L. B., and Michailos, K. Local earthquake monitoring with a low-cost seismic network: a case study in Nepal. *Earth, Planets and Space*, 76(1): 116, 2024. doi: https://doi.org/10.1186/s40623-024-02047-y.

Tian, D., Uieda, L., Leong, W. J., Schlitzer, W., Fröhlich, Y., Grund, M., Jones, M., Toney, L., Yao, J., Magen, Y., Tong, J.-H., Materna, K., Belem, A., Newton, T., Anant, A., Ziebarth, M., Quinn, J., and Wessel, P. PyGMT: A Python interface for the Generic Mapping Tools. doi: 10.5281/zenodo.8303186.

Upton, E. and Halfacree, G. *Raspberry Pi user guide*. John Wiley & Sons, 2016. doi: 10.1002/9781119415572.

Wessel, P., Luis, J. F., Uieda, L., Scharroo, R., Wobbe, F., Smith,

W. H. F., and Tian, D. The Generic Mapping Tools version 6. *Geochemistry, Geophysics, Geosystems*, 20(11):5556–5564, 2019. doi: https://doi.org/10.1029/2019GC008515.

Williams, C. A., Eberhart-Phillips, D., Bannister, S., Barker, D. H., Henrys, S., Reyners, M., and Sutherland, R. Revised interface geometry for the Hikurangi subduction zone, New Zealand. *Seismological Research Letters*, 84(6):1066–1073, 2013. doi: https://doi.org/10.1785/0220130035.

Winter, K., Lombardi, D., Diaz-Moreno, A., and Bainbridge, R. Monitoring icequakes in East Antarctica with the raspberry shake. *Seismological Society of America*, 92(5):2736–2747, 2021. doi: https://doi.org/10.1785/0220200483.